Optik - International Journal for Light and Electron Optics 235 (2021) 166636

Contents lists available at ScienceDirect

Optik

journal homepage: www.elsevier.com/locate/ijleo

Original research article

Sustainable preparation of ixora flower-like shaped luminescent powder by recycling crab shell biowaste

M.V.S. Rezende [a,*], U.C. Pereira [b], Y.R.R.S. Rezende [b], I.S. Carvalho [a], W.S. Silveira [a], D.O. Junot [c], R.S. Silva [a], C.X. Resende [d], N.S. Ferreira [a]

[a] Departamento de Física, Universidade Federal de Sergipe, 49100-000, SE, Brazil
[b] Laboratório de Flavor, Universidade Federal de Sergipe, 49100-000, SE, Brazil
[c] Instituto de Pesquisas Energéticas e Nucleares, SP, Brazil
[d] P2CEM, Universidade Federal de Sergipe, 49100-000, SE, Brazil

ARTICLE INFO

Keywords:
Luminescence
Powder
Recycle
Crab shell

ABSTRACT

We report on cost-effective recycling of crab shell biowaste and synthesis of luminescent powders. XRD, thermogravimetric and, FTIR analysis revealed that calcination temperature must be beyond ~800 °C to recycle biowastes crab (*Ucides cordatus*) shell into crystalline powder composed of CaO, and a small amount of $CaCO_3$, $NaCa(PO_4)$, MgO, and $Ca_{10}(PO_4)_6(OH)_2$. SEM analysis revealed that calcination of crab shell biowaste at 800 °C/2 h produced the homogeneous cauliflower- and ixora flower-like shaped intrinsic luminescent powders. XEOL and thermoluminescence analyses suggest that F^+-centers of the CaO structure are responsible for the efficient intrinsic scintillation of the crab shell powder. Therefore, our study shows a biomaterial promise derived from seafood wastes as natural dosimeter materials for industrial applications.

1. Introduction

The seafood consumption has increased considerably on a worldwide scale because it is an important source of nutrients for human health. Most of the marine invertebrates that are widely being used as food produce significant waste during their industrial processing. Among several marine invertebrates, crabs are estimated to account for the current major waste production. The annual discard of crab waste worldwide is estimated to be 6–8 million tons [1]. Most of these biowastes are either buried or burned, which has become a considerable environmental secondary pollution trouble nowadays. Therefore, cost-effective strategies that recover crab waste into commercial interest products are largely demanded to reduce the volume of this biowaste, minimizing this secondary pollution problem. Recently, crab shell waste has attracted considerable interest of researchers because it can be recycled into inexpensive and renewable functional materials. It has been revealed that crab shell wastes are rich in various protein and amino acids, calcium, carotenoids and, chitin [2]. Additionally, recent researches show that crab shell as seafood waste has been used as source of chitin, calcium phosphate-based-hydroxyapatite powders, and metal removal from aqueous solutions [3]. Nevertheless, these uses do not provide a wide range of alternatives for all crab shell waste, and its intrinsic benefits to developing new technologies are still lacking. This letter attempts to fill this gap by promoting a future sustainable crab shell waste recycling into valuable intrinsic luminescent powder. Herein, crab shells(*Ucides cordatus*) were washed and dried, and thereafter, the dried sample was thermally

* Corresponding author.
E-mail address: mvsrezende@gmail.com (M.V.S. Rezende).

https://doi.org/10.1016/j.ijleo.2021.166636
Received 22 January 2021; Accepted 25 February 2021
Available online 1 March 2021

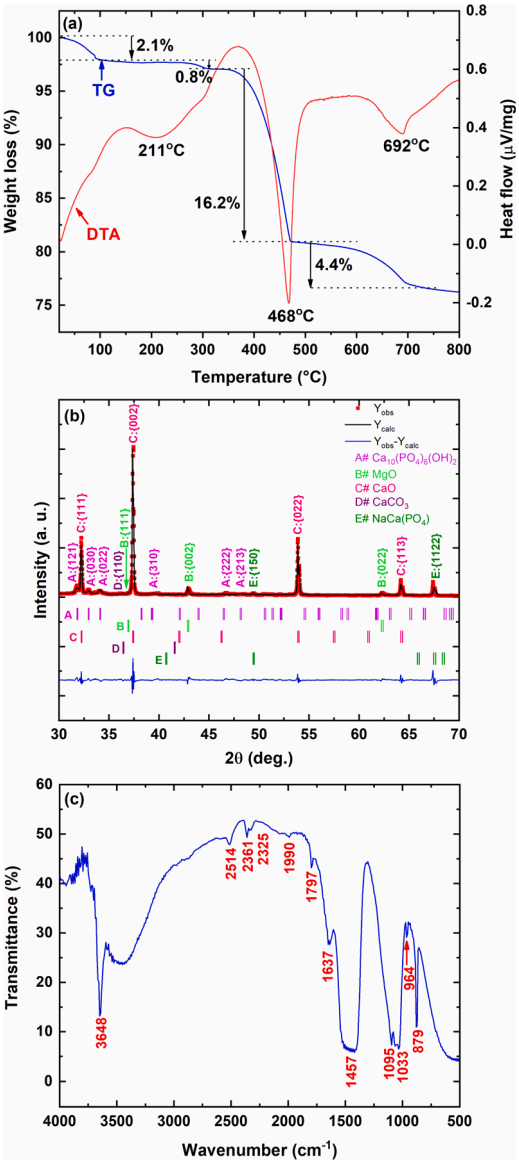

Fig. 1. (a) TG-DTA of the crab shells before heat treatment. (b) experimental and whole pattern fitted XRD pattern and (c) FTIR spectrum of the crab shells after calcination.

treated. The chemical, structural, morphological, and optical properties of the calcined crab shells powder was investigated to determine its possible application as futuristic phosphor materials for dosimetric detectors.

2. Methodology

Initially, the waste of crabs shells(*Ucides cordatus*) species was taken from a bar located at Atalaia beach in Aracaju city, Sergipe State, Brazil. The waste of crab's shells was washed with water and then calcined at 800 °C for 2 h. Before any further treatments, the dried crab's shells were analyzed by thermogravimetric and differential thermal analyses (TGA-DTA, ETZSCH STA-449F1-Jupiter). Finally, the calcined crabs' shells powder was investigated by X-ray diffraction (XRD, Bruker-Adcance) using Cu-Kα radiation, 40 kV, and 40 mA, 30−70º(2θ), 0.02°/min. The XRD pattern was refined using a "whole pattern fitting" algorithm, as implemented in the Fullprof software [4]. Fourier transforms infrared (FTIR) spectrum was obtained by using a spectrophotometer (Varian, 640IR). SEM image was performed on scanning electron microscope (JEOL JSM-5700, 10 kV). TL and OSL analyses were performed in a Risö TL/OSL reader. X-ray excited optical luminescence (XEOL) spectrum was measured at the XAFS2 beamline at the Brazilian Synchrotron Light Laboratory-LNLS.

Table 1
Lattice parameters and phase content of inorganic oxides present in the calcined crab shells powder.

Compound	space group	lattice parameters		Phase content(%)
		a, b	*c*	
$Ca_{10}(PO_4)_6(OH)_2$	$P6_3/m$	9.414553	6.875983	19.4
$NaCa(PO_4)$	*Pn21a*	20.396999, 5.412000	9.161001	2.5
$CaCO_3$	R -3 c	5.018342	13.514201	5.0
CaO	Fm-3 m	4.808956	4.808956	65.1
MgO	Fm-3 m	4.215889	4.215889	8.0

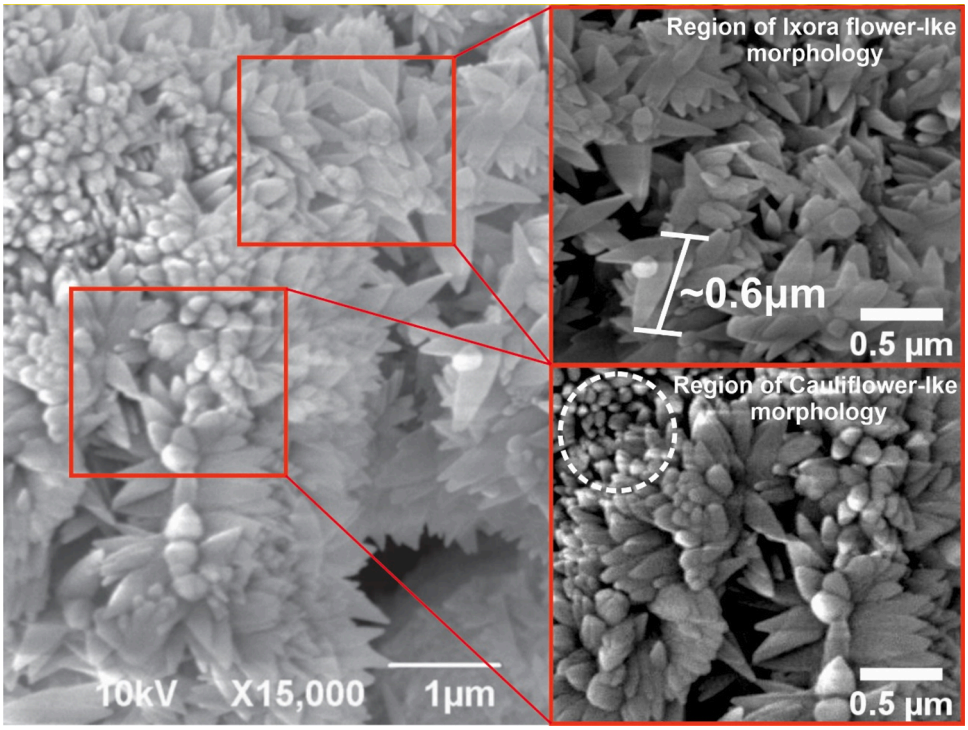

Fig. 2. SEM image of calcined crab shells powder.

3. Results and discussion

TGA-DTA analysis reveals that crab shell powder continually lost weight in three stages (Fig. 1(a)). Firstly, the small weight losses of 2.1 % and 0.8 % followed by endothermic peaks at 211 °C in the DTA curve are attributed to removing absorbed water from the carbonate lattice. Secondly, the considerable weight loss (~16.2 %) accompanied by an endothermic peak at ~468 °C is indicative of the thermal decomposition reactions of biologics compounds, mainly the polymerization and dehydration of saccharide rings, as well as depolymerization of chitin. Finally, the 4.4 % weight loss represented by the endothermic peak at ~692 °C indicated most likely decomposition of $CaCO_3$ to CaO with the release of CO_2 and higher hydroxyapatite crystallinity and other minerals in crab shells. The significant thermal decomposition ended at about 800 °C.

Fig. 1(b) shows the XRD pattern refined using a "whole pattern fitting" of the crab shells powder. All peaks can be indexed to magnesium oxides(MgO, ICSD#60692), calcium oxides(CaO, ICSD#26959), calcium carbonate($CaCO_3$, ICSD#18165), sodium calcium phosphate ($NaCa(PO_4)$, ICSD#35629) and hydroxyapatite ($Ca_{10}(PO_4)_6(OH)_2$, ICSD#016742). The whole pattern fitting results showed that the structural parameters were in close agreement with the ICSD cards, as given in Table 1. Moreover, it is revealed 65.1 % of CaO and 19.4 % of $Ca_{10}(PO_4)_6(OH)_2$ as majors phases and also minors phases such as MgO(8.0 %), $NaCa(PO_4)$(2.5 %) and, $CaCO_3$(5.0 %). The well-recognized main components of crab shells are $CaCO_3$ [5]. Thus, these results suggest that amounts of $CaCO_3$ present in the crab shell powder were converted into CaO by decarboxylation [6].

The FTIR spectrum of the crab shells powders shows bands attributed to hydroxyl, and different types of carbonate and phosphate (Fig. 2(b)). The bands at 879 and 1457 cm^{-1} are assigned to ν_2 and ν_3 mode of CO_3^{2-} of $NaCa(PO_4)$ and type-B $Ca_{10}(PO_4)_6(OH)_2$ [7], respectively. Others bands at 1797, 1990 and, 2514 cm^{-1} are attributed to the stretching vibrations of CO_3^{2-}in the IR region. The IR band at 2361 cm^{-1} associated with the symmetric axial deformation of the CO_2. The ν_1-symmetric stretching mode of PO_4^{3-} is obtained

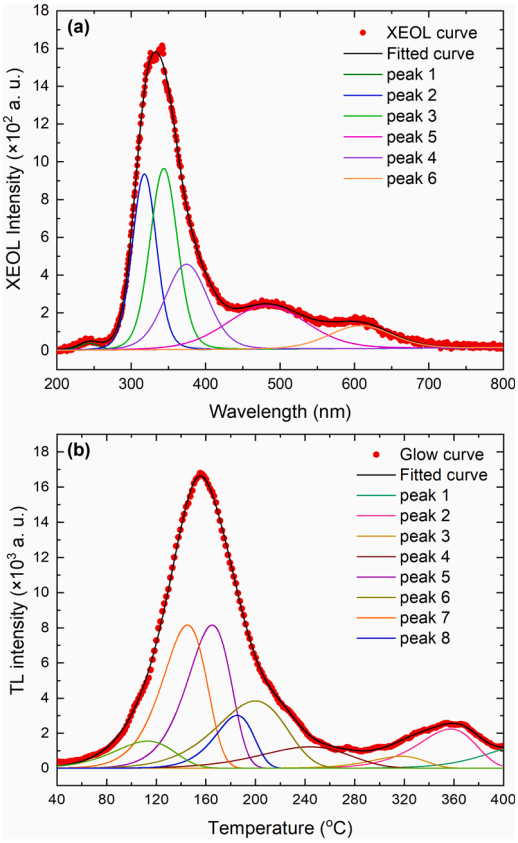

Fig. 3. Deconvoluted (a) XEOL and (b) TL glow curve of the calcined crab shells powder.

at 964 cm^{-1}, and ν_3 P–O asymmetric stretching modes related to orthophosphate groups are 1033 and 1095 cm^{-1} [8]. The broad peak approximately 3648 cm^{-1} depicts the stretching mode of the OH^- bands, indicating the formation of hydrogen-bonded H_2O due to the water adsorption by CaO [9]. Finally, the band at 1637 cm^{-1} corresponds to OH— stretching vibration from residual water on the sample [10]

The SEM image reveals that the sample is composed by agglomerated microstructures forming cauliflower and ixora flower-like morphologies. The cauliflower morphology of the crab shell powder may be attributed to the calcining process-induced volatilization of organic materials and releasing of CO_2during the $CaCO_3$ decomposition to form CaO. Nevertheless, ixora flower-like morphology formed of oblong microstructures ~0.6 μm long, carried in opposite pairs that forms dense rounded clusters across. This is a result of the intrinsic (002) face preferential growth of $Ca_{10}(PO_4)_6(OH)_2$, which favors the formation of rods rather than particles [11]. EDS of the calcined powder indicates the presence of a higher amount of distributed calcium (30.26at.%) and oxygen (53.63at.%), as compared to carbon (8.58at.%), sodium (1.19 at.%), magnesium (4.27at.%) and, phosphorous(2.04at.%).

Fig. 3 (a) shows the deconvoluted XEOL emission spectrum when excited at 7000 eV. The peak at around 243.6 nm corresponds to the charge-transfer transition within the PO_4^{-3} groups in the $Ca_{10}(PO_4)_6(OH)_2$ structure [12]. The 317.8 nm emission peak is the $^2T_{1u}$(x, z)→$^2A_{1g}$ transitions from the F^+-center in the CaO structure [13]. The uncommon emission at 374.2 nm is associated to an F^+-center interaction with two neighboring magnesium impurities on opposite sides of an oxygen vacancy in the CaO lattice [14].The peak at 481.9 nm corresponds to $^1T_{1u}$→$^1A_{1g}$ transition, which can be attributed to F-center (two electrons rapped at O^{2-} vacancies) in the CaO structure [15]. The peaks at 357.1 nm and 608.4nm [13] corresponds to the $^2T_{1u}$(y)→$^2A_{1g}$ and $^3T_{1u}$→$^1A_{1g}$ transitions, which are attributed to fluorescence from the self-absorption of photons emitted from the F^+-centers and F-centers in the CaO, respectively. Herein, the F^+-center was generated due to the high energy excitation during the XEOL measurement. The TL glow curve obtained after irradiation with 800 mGy from a $^{90}Sr/^{90}Y$ beta source at a heating rate of 10 °C/s for the crab shells powder are shown in Fig. 3(b). The deconvolution of the TL curve into eight peaks was performed using a best-fit procedure and the first-order kinetics model (FOM~2.6 %) [16]. The decomposition and conversion of $CaCO_3$ into CaO when the crab shell powder was irradiated and heated up to 400 °C results in the evaporation of several gaseous of different symmetries such as CO_2^-, CO_3^{3-}, CO_3^-, CO^- and O^-, as seen from the FTIR spectrum. The emission peaks at 124, 153.7, and 251.9 °C are possibly due to surface (or grain boundaries) defects, O ion and F^+-center recombination and, radiation induced CO_3^{2-}radicals in $CaCO_3$, respectively. The relatively broadening peaks at 188.6 and 363.2 °C are attributed majority to hole trapped at PO_4^{3-}radicals and neutral electron traps induced by recombination of radiation-induced CO_2^- radicals, located both in the $OH^-$and PO43− sites of the $Ca_{10}(PO_4)_6(OH)_2$, lattice and on the surface on the Ca_{10}

$(PO_4)_6(OH)_2$ and $NaCa(PO_4)$ surface [17], respectively. The displacement of a O^{2-} ion in the cubic structured CaO and MgO oxides favors the formation of two stable electron centers. Thus, the 213 °C is assigned to F^+-centers formed as a result of electron-trapped by oxygen vacancies in MgO [18]. Furthermore, peaks at 170.1 and 338 °C are associated with two electrons trapped at O^{2-}vacancies (F-center) in the CaO lattice [15]. Therefore, we can see reasonable stability, whereas the peak at 213 °C for MgO is more intense and thermally stable than the one at 338 °C for CaO. This result suggests that that the peak at 213 °C for MgO in crab shell powder can be suitably used as a dosimetric peak.

4. Conclusion

In summary, we synthesize luminescent powders by recycling of crab shell biowaste (*Ucides cordatus*). XRD, thermogravimetric and, FTIR analysis revealed that biowastes crab shell recycled into an intrinsic luminescent crystalline powder composed of CaO, $CaCO_3$, $NaCa(PO_4)$, MgO, and $Ca_{10}(PO_4)_6(OH)_2$ by calcination at ~800 °C. SEM images revealed that the calcined crab shell powder shows both cauliflower- and ixora flower-like shaped morphologies. XEOL and TL analyses suggest that F^+-centers of the CaO structure is responsible for the efficient intrinsic scintillation of the crab shell powder. Therefore, our study shows that biomaterial derived from seafood wastes can be a promising aspirant for industrial applications.

Declaration of Competing Interest

The authors report no declarations of interest.

Acknowledgments

The authors are grateful to the Brazilian Funding Agencies: FINEP, CAPES, and CNPq(407261/2018-4). They also thank the XAFS2 (Proposal#20190084) beamlines from the LNLS.

References

[1] N. Yan, X. Chen, Nature 524 (7564) (2015) 155–157.
[2] F.C. Meldrum, Int. Mater. Rev. 48 (3) (2003) 187–224.
[3] B.N. Bhattacharjee, V.K. Mishra, et al., ACS Omega 4 (7) (2019) 12753–12758.
[4] J.R. Carvajal, Newsletter 26 (2001) 12–19.
[5] F. Boßelmann, P. Romano, et al., Thermochim. Acta 463 (1) (2007) 65–68.
[6] F. Peters, K. Schwarz, et al., Thermochim. Acta 361 (1) (2000) 131–138.
[7] A. Doostmohammadi, A. Monshi, et al., Ceram. Int. 37 (7) (2011) 2311–2316.
[8] A. Destainville, E. Champion, et al., Mater. Chem. Phys. 80 (1) (2003) 269–277.
[9] T. Witoon, Ceram. Int. 37 (8) (2011) 3291–3298.
[10] A.P.D.S. Pereira, M.H.P.D. Silva, et al., Mater. Res. 20 (2017) 411–420.
[11] V.K. Mishra, B.N. Bhattacharjee, et al., J. Alloys. Compd. 614 (2014) 283–288.
[12] C. Yang, P. Yang, et al., J. Colloid Interface Sci. 328 (1) (2008) 203–210.
[13] J. Carrasco, C. Sousa, et al., J. Chem. Phys. 125 (7) (2006), 074710.
[14] A.E. Hughes, G.P. Pells, J. Phys. C Solid State Phys. 8 (21) (1975) 3703–3709.
[15] Y. Jin, Y. Hu, et al., Mater. Sci. Eng. B 178 (18) (2013) 1205–1211.
[16] M. Puchalska, P. Bilski, Radiat. Meas. 41 (6) (2006) 659–664.
[17] C.E. Secu, M. Cherestes, et al., Radiat. Meas. 46 (10) (2011) 1109–1112.
[18] J.E. Wertz, P. Auzins, et al., Phys. Rev. 107 (6) (1957) 1535–1537.